

Trapping and detrapping of electrons photoinjected from silicon to ultrathin SiO₂ overlayers. I. In vacuum and in the presence of ambient oxygen

N. Shamir,^{a)} J. G. Mihaychuk,^{b)} and H. M. van Driel^{c)}

Department of Physics, University of Toronto, Toronto, Ontario M5S 1A7, Canada

(Received 5 January 2000; accepted for publication 15 April 2000)

Transient trapping/detrapping of electrons at the Si(100)/SiO₂ outer surface is studied in vacuum or with an O₂ ambient (between 10⁻³ and 30 Torr) following internal electron photoemission from Si. Photoemission-current (produced by a 150 fs, 800 nm laser source) and contact-potential-difference techniques were used to investigate a wide variety of *n*- and *p*-doped samples at 300 K with thermally grown, steam grown, and dry oxides with thickness ≤5 nm as well as samples with the oxide layers removed. Characteristics of the steam grown oxide were also studied at 400 and 200 K. For samples in vacuum charging is attributed to direct filling of at least two families of traps, one related to the oxide and the other the Si/SiO₂ interface. For samples in O₂, details of oxygen-assisted surface charging as reported previously [Phys. Rev. Lett. **77**, 920 (1996)] are given. A fast, Coulomb-repulsion driven spillover of surface charge from the irradiated spot to the rest of the surface was detected. Oxygen aids trap filling of the in-vacuum filled and gas-sensitive traps and also detrapping (the efficacy of which increases strongly from 400 to 200 K) when the optical excitation source is removed. Surface transient charging and charge trapping efficacy for the oxidized samples are not very sensitive to sample preparation. A mobility of the trapped charges, probably hopping between traps and also Coulomb-repulsion driven, was measured. © 2000 American Institute of Physics. [S0021-8979(00)05114-8]

I. INTRODUCTION

Charge trapping and detrapping phenomena at oxidized silicon surfaces are of fundamental interest as well as of crucial importance to silicon device technology. For example, the development of submicron metal-oxide semiconductor (MOS) structures is highly dependent on the development of device-quality ultrathin (5 nm thick or less) MOS gate dielectrics^{1,2} and charge accumulation within these layers is harmful to performance. Charge transfer from Si to SiO₂ via thermionic or photoemission is also known to be important in thermal oxidation of Si.^{3,4} The characterization of the oxide traps has long been dominated by capacitance-voltage (*C-V*) and current-voltage (*I-V*) measurements in MOS structures.^{5,6} However, optical techniques, especially those based on femtosecond pulse sources for which nonlinear optical effects can be achieved with minimal sample heating,⁷ have been shown to provide high temporal, spatial, and spectral resolution capabilities for studying Si/SiO₂ systems.⁷⁻¹⁹ Recently we have shown that electric-field-induced optical second-harmonic generation (EFISH) and multiphoton photoemission (MPPE) current techniques present a more versatile method than *C-V* or *I-V* for mea-

suring charge accumulation at the oxide surface, in oxide traps and at adsorbed gas-phase species in the Si/SiO₂/ambient-gas system.^{8,11,15}

Figure 1 illustrates the essential physical phenomena in MPPE experiments. Intense laser radiation with photon energy 1.55 eV transfers electrons from bulk silicon via three photon photoemission (3PPE) or four photon photoemission (4PPE). In the former case, which we refer to as internal photoemission (IPE), electrons can transfer to the external interface and become trapped. For simplicity, emission from donor levels and mid-gap states (which are a minority) are omitted in the scheme, but can take place as well. Since the threshold energy of silicon is²⁰ ≈5.15–5.40 eV, electrons can be photoemitted from the solid via external photoemission if they are excited via 4PPE from the Si valence band (VB), or by 3PPE (in the case of previously excited electrons or doped materials) from the conduction band (CB). The separation of charge establishes electric fields up to 1 MV/cm which can be monitored via EFISH or through the change in the work function as measured by MPPE. Although both techniques require independent calibration of the magnitude of the associated electric field or work function the changes in these parameters can be directly used to monitor charge dynamics. In particular we have demonstrated²¹ how both techniques illustrate the role of oxygen in assisting charging of the oxide layer following IPE. MPPE is sensitive for O₂ pressure, *P* < 10 Torr with EFISH usable at higher pressure. In this article we also use MPPE to perform detailed studies of how oxygen assists charge trapping and detrapping from oxidized silicon wafers

^{a)}Permanent address: Nuclear Research Center-Negev, P.O. Box 9001, Beer-Sheva, Israel.

^{b)}Present address: DALSA Inc., 605 McMurray Rd., Waterloo, ON N2V 2E9, Canada.

^{c)}Corresponding author, electronic mail: vandriel@physics.utoronto.ca

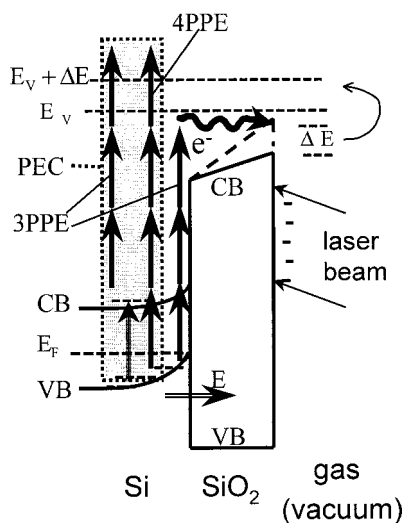


FIG. 1. Schematic diagram of the MPPE processes.

prepared under a variety of conditions and we separate ambient O_2 effects from intrinsic (direct) charge trapping effects as occur for samples in vacuum. Because optical techniques are unable to directly measure absolute values of work function (WF) changes, a Kelvin probe (KP), measuring WF changes by the contact-potential-difference (CPD) method²² was also used. The introduction of the CPD method in this study (unlike the previous one²¹) enabled looking at adsorption phenomena without the laser beam effect and also outside its area, which is not possible by the former techniques since the laser beam serves both as pump as well as probe.

The remainder of this paper is organized as follows. In Sec. II we briefly review the experimental techniques and give sample characteristics. In Sec. III we give experimental results, which are analyzed and discussed in Sec. IV, and the conclusions are given in Sec. V. In a subsequent paper we will discuss the role of other gases in assisting charging effects on silicon. Oxygen is seen to be a special case since it not only appears to catalyze charging and trapping effects, as do other gases, but it also leads to charge accumulation on the surface.

II. EXPERIMENTAL TECHNIQUES AND SAMPLES

The overall experimental setup is presented in Fig. 2. The vacuum chamber is equipped with various diagnostic tools including mass and Auger spectrometers. The base vacuum in the measurement chamber was usually in the low 10^{-8} Torr range, but to ensure that no residual gas effects are present some of the experiments were repeated in the 10^{-10} Torr range. The samples were irradiated by 150 fs pulses with energies $3 \mu\text{J}$ from a 250 kHz regeneratively amplified Ti:sapphire laser source operating at $\lambda = 800 \text{ nm}$ (1.55 eV) producing a peak irradiance of up to 30 GW/cm^2 in a spot of diameter $\sim 100 \mu\text{m}$ spot on the sample. A picoammeter connecting the sample to ground and monitored by a computer provided a measurement of the net current from the sample by recording the (positive) compensating current of equal magnitude to the photoemission current (PEC). Currents (produced by MPPE) of up to several nA

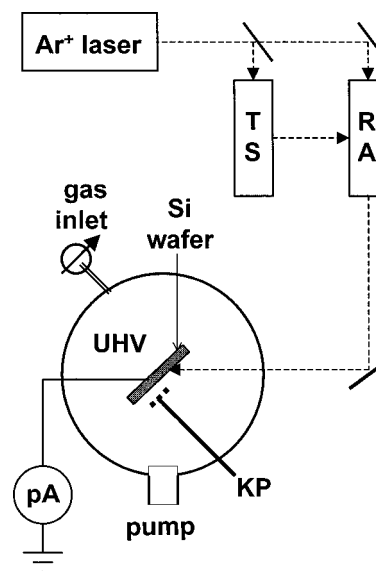


FIG. 2. A diagram of the layout used for photoemission-current and work function measurements. TS—Ti:sapphire laser; RA—regenerative amplifier; UHV—ultrahigh-vacuum chamber; KP—Kelvin probe; and pA—picoammeter.

(10^{14} electrons/ cm^2/s) were observed. The mean free path of an electron emitted by 3PPE (4.65 eV) or 4PPE (6.2 eV) in the silicon is $\sim 10 \text{ nm}$ according to the universal experimental curve.²³ The measured PEC was maximum for 5 nm thick oxide and not significantly larger for clean Si, indicating that photoelectrons are efficiently emitted from the Si through the oxide for samples having oxides a few nanometers thick. The Kelvin probe²⁴ consists of a 2.5 mm diameter mesh, which monitors an area $\sim 10^3$ times larger than that of the laser irradiated spot. Since the processes inside the spot yield WF changes smaller than 1 eV ,⁹ the KP is not sensitive to processes confined only to the irradiation area. Therefore, it cannot serve to absolutely calibrate the MPPE monitored processes. Since no lateral resolution of the WF changes taking place outside the irradiated spot is available, the KP yields the average value of the WF on the whole surface. Since the KP is not sensitive to processes that are confined to the laser irradiated spot, the latter was placed $1\text{--}3 \text{ mm}$ below the area monitored by the KP in order to ensure that no direct interaction between the probe and the laser beam occurs. No significant change in the CPD measured when changing the distance between the KP and irradiated beam was observed, and it is assumed, therefore, that the KP measures WF changes that occur on the whole surface (outside the irradiated spot). As can be expected, the KP, being a vibrating biased electrode near the surface, affects the PEC, the effect being larger for the lower energy MPPE. Therefore, no use was made of the PEC measurements that were performed simultaneously with the CPD ones for calculating relative PEC intensities or WF changes. However, the simultaneous measurements provide essential information about relative time constants and comparative behavior in and outside the laser beam spot. For unaffected PEC, to be compared to the CPD, separate measurements were conducted, using the same experimental conditions. The sample temperature could

be varied using liquid nitrogen flow or resistive heating (not during PEC measurement) over a temperature range from 200 to 400 K.

The samples were chosen so that the effect of such parameters as the presence of an oxide, its thickness, and method of preparation, as well as the silicon doping on the studied processes, could be determined. Several *n*-Si(001) and *p*-Si(001) samples were used. All samples were taken from polished, optically smooth wafers and had a surface area of $\sim 2 \times 12 \text{ mm}^2$ and thickness 0.3 mm. Since the studies presented indicate that the relevant parameter for most results is the type of oxide (rather than amount of doping, at least for levels below 10^{18} cm^{-3}), the oxide thickness and preparation method, and type of doping will denote the samples. The samples used are (a) 15Sn: $a \sim 1.5 \text{ nm}$ oxide film grown in steam at 850 K on a low-doping *n*-Si(001) substrate (resistivity 20–100 $\Omega \text{ cm}$); (b) 50 Dn: a 5.0 nm oxide grown in dry O_2 at 1000 K on *n*-Si(001) (resistivity 20–100 $\Omega \text{ cm}$); (c) HFSn: HF partially etched 15Sn sample; (d) 10 Ap: a 1.0 nm oxide layer produced by anodic oxidation using 0.1 M HCl with a low-doping (resistivity 3–7 $\Omega \text{ cm}$) *p*-Si(001) substrate; (e) CLn: the oxide of a 15Sn sample was removed (in UHV) by resistive heating at 1400 K (cleanliness checked by *in situ* Auger electron spectroscopy); and (f) CLp: a 10 Ap sample, the oxide of which was removed by the same method as in (e). Both clean Si surfaces were passivated by a long exposure to oxygen (forming a chemisorbed layer), so further gas admission resulted in reversible CPD values. As shown below, since the PEC at the end of a measurement did not recover to the initial value due to long-lifetime trap states, the initial conditions were restored by heating the sample to $\sim 900 \text{ K}$ in vacuum for several minutes before allowing samples to cool to room temperature. It should be noted that the initial intensity of the PEC can vary by as much as an order of magnitude for different surface locations. This and other measurements' variation with surface position will be discussed later. Unless otherwise indicated, the initial behavior of the PEC represents the common behavior for all the samples.

III. RESULTS

Here we present the salient features of the MPPE and CPD experiment. We defer an extensive interpretation and discussion of the results to the following section. We begin by considering the photoinduced charge trapping in the various samples under vacuum ($< 10^{-8} \text{ Torr}$) conditions.

A. Samples in vacuum

Figure 3 presents PEC measurements on the various samples (including two measurements on the 15Sn sample after different treatments). In most cases, following commencement of laser excitation of the sample, a fast decrease of PEC is observed followed by a much slower decrease. The magnitude and time scale of this decrease changes from spot to spot and from sample to sample. The PEC intensities were normalized to unity at 100 s (so the slow-decrease component of the signal is comparable for all the samples) and shifted for convenience. The effect of the laser beam appears to be confined to the illumination spot. Moving the sample a

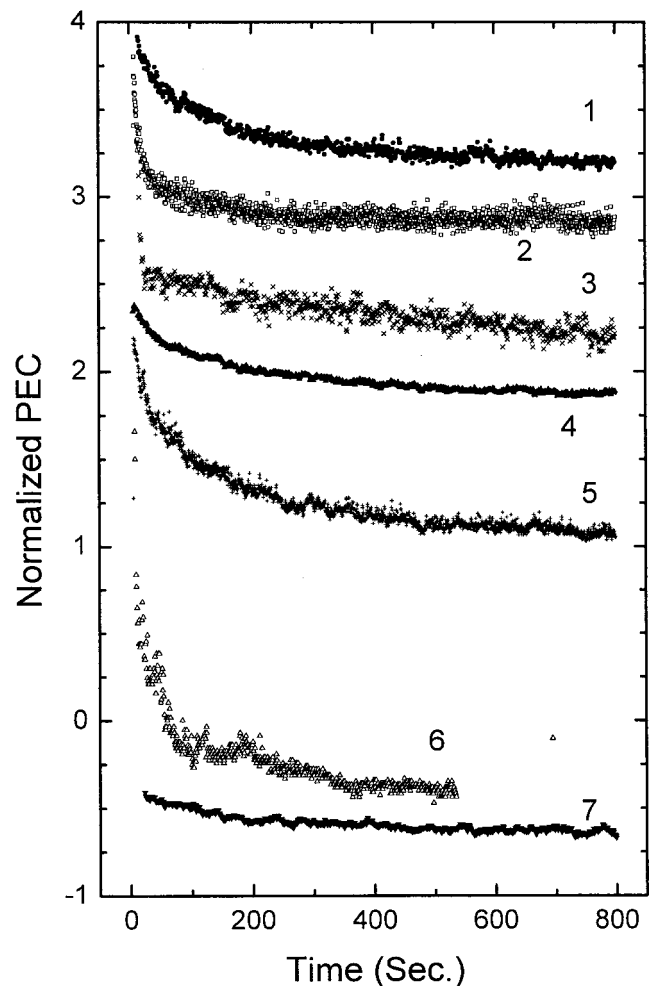


FIG. 3. Normalized time-dependent PEC signal illustrating typical direct filling process on the different samples: (1) 15Sn; (2) 15Sn after ~ 5 heating ($\sim 900 \text{ K}$)-cooling cycles; (3) HFSn; (4) CLn; (5) 50Dn; (6) 10Ap, and (7) CLp.

few tens of microns relative to the laser beam gives photoemission characteristics similar to a virgin sample. This indicates that the mobility of trapped charges leading to work function changes is small and/or slow. However, from measurements of the type shown in Fig. 3 but at different sample spots we note a lateral variation of initial PEC. Indeed for some spots the PEC does not decrease.

As mentioned before, EFISH and PEC measurements are unable to determine whether immediate transient-surface-charging also occurs in vacuum, or ambient gas is needed for this process. This is because the laser beam serves as both pump and probe. A CPD measurement before and after beam illumination can answer this question. The reaction to the laser irradiation (for a grounded sample) is an immediate drop in the CPD of $\sim 0.1 \text{ eV}$ (see Fig. 11 below), reaching an immediate steady state (SS), and recovering almost immediately when the laser beam is turned off. For a floating sample a similar effect, albeit 50 times larger, occurs. This is attributed to a compensating current to the PEC, reaching a SS that is equal in intensity, but slightly delayed. Therefore, a small potential difference is maintained, acting as a continuous driving force to the compensating current. For a floating

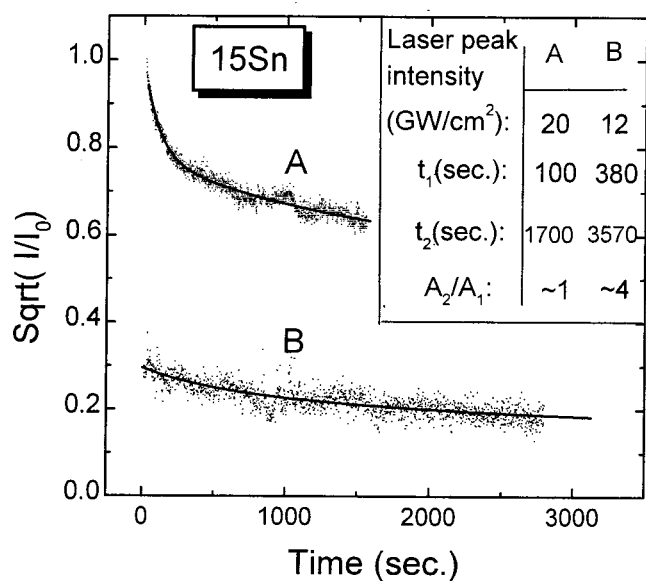


FIG. 4. The dependence of DF decay times on the laser peak intensity. I —PEC intensity. $I_0 = I(t=0)$. Best-fit curves for a two-exponential decay function are plotted, the decay times and the ratio of the preexponents are indicated. The curves were shifted for convenience

sample the effect is strongly increased since compensating the PEC depletes the neighboring free electron reservoir (of the metallic sample holder and the attached cables) thus being driven by a much higher potential difference. This CPD drop is only weakly dependent on the laser intensity, as opposed to an expected MPPE-driven transient surface charging, and is also in the opposite direction, apparently not pointing to vacuum surface charging. Since the CPD drop is immediate, neither the PEC nor the EFISH are affected by it, having the new SS as their starting point. In some cases, however, this SS is not reached immediately, and the PEC increases before reaching the SS.

Figure 4 shows how the PEC current varies with laser irradiance. It is clear that the temporal characteristics are nonexponential and dependent on laser irradiance. A two-exponential function, at least, is needed to fit the PEC curve; such a fit is presented in the figure. The very different dependence of the two time constants on irradiance points to different processes as will be discussed in Sec. IV A.

B. Samples in oxygen

Figure 5 presents a series of PEC measurements for different O₂ exposures at various pressures of the (a) 15Sn and (b) CLn samples. After gas removal in an illumination and exposure sequence, the PEC has a value significantly lower than the initial one. The same measurement sequences for the 10Ap and CLp samples (not presented) are essentially the same as for 15Sn and CLn, respectively. Figure 6 illustrates the normalized PEC for the different samples under the same illumination/exposure sequence as in Fig. 5. For all samples, an immediate (pressure dependent) decrease in intensity of the PEC, when the beam is turned on, is followed by a slower (also pressure dependent) decrease in intensity until saturation (or nullification) occurs. When the gas is pumped

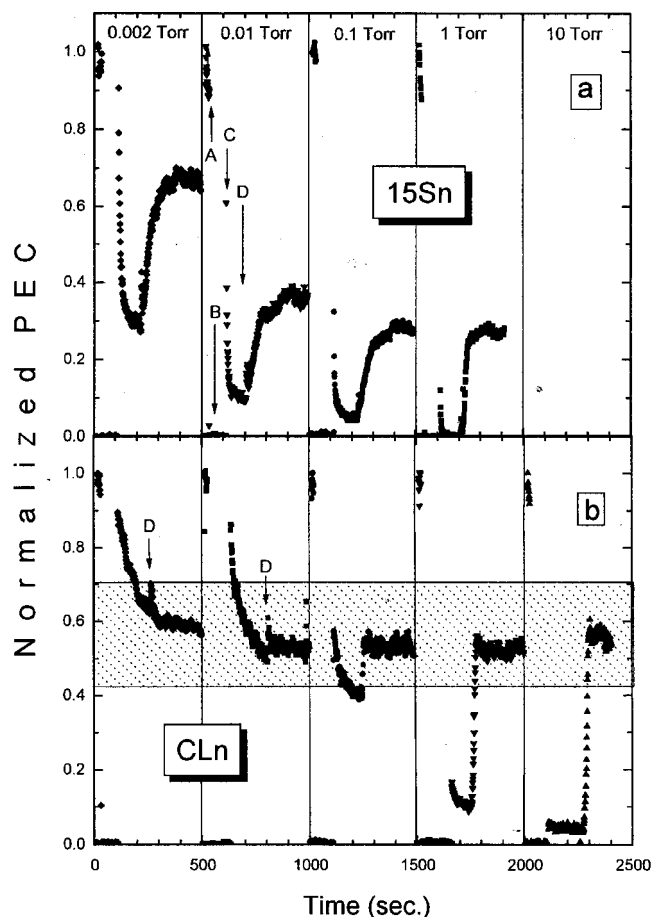


FIG. 5. Photoemission current (PEC) measurement sequences before, during, and following exposures to various oxygen pressures (shifted in time, for convenience) for (a) 15Sn: A—beam off, B—gas admission, C—beam on, D—gas pumping; (b) CLn, the dashed area presents the range of direct filling saturation for different spots on this sample.

out, some recovery of the PEC intensity occurs, but the current does not reach the initial intensity. The specifics, however, are different for the different samples, as can be seen for the examples presented in Figs. 5 and 6. Note that accumulation of gas exposure (without laser beam on) has no apparent effect. The initial current drop as well as the slower ensuing drop are independent of the time and pressure of exposure to the gas when the beam is blocked. The final PEC (as well as the final EFISH signal^{8,15,21}) after a sequence of gas exposure in the presence of the laser beam is always lower (higher) than the initial one (as can be observed in Figs. 5 and 6), i.e., a residual effect is present. This residual effect is very stable (up to days). Its removal, as mentioned earlier, is achieved by heating the sample to ~900 K for a couple of minutes. Using high gas doses (e.g., $P > 1$ Torr for > 100 s, or 30 Torr for even shorter times) while the beam is on, a saturation level of the PEC is achieved. It was noticed that after many heating/cooling sequences this residual PEC is significantly lower than that for a virgin sample.

The effect of the laser beam, combined with gas exposure, appears to be confined to the vicinity of the spot of laser illumination. By moving the sample a few tens of microns relative to the laser beam, one obtains a new measure-

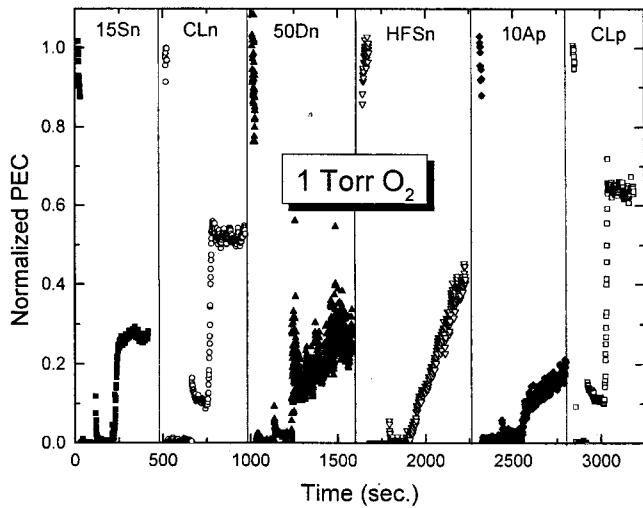


FIG. 6. The PEC measurement sequences before, during, and following exposures to 1 Torr O₂ for the various studied samples.

ment spot with photoemission characteristics of a virgin sample. For oxide covered samples, this is true for a few minutes after which a diffusionlike effect starts to affect the vicinity of the illumination spot (see Sec. IV F). For the clean Si samples (CLn and CLp) this mobility effect does not seem to occur. Exposure sequences, measured using different laser powers, always exhibit the instantaneous initial decrease in current intensity when the gas is applied.

Figures 7 and 8 present effects of temperature on the

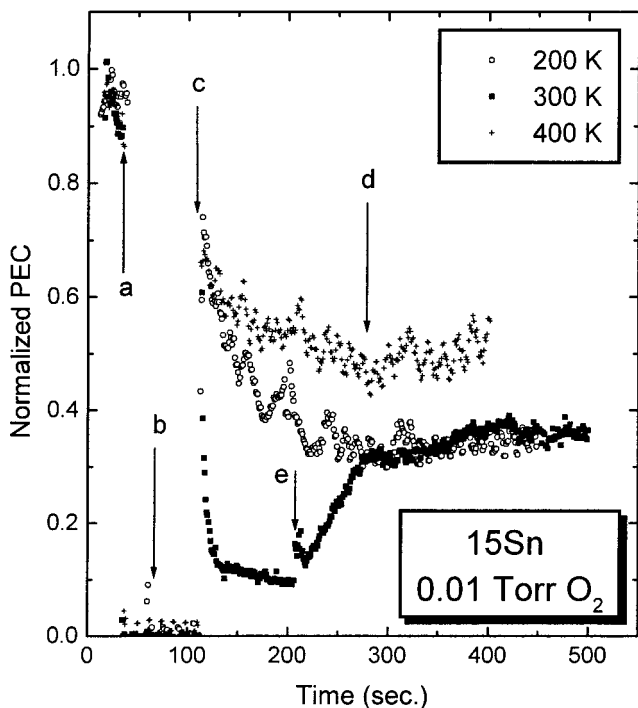


FIG. 7. Gas exposure/illumination sequence for sample 15Sn and an O₂ pressure of 0.01 Torr at temperatures 200, 300, and 400 K. a—beam off; b—gas admission; c—beam on; d—pump-out for 400 and 200 K; and e—pump-out for 300 K.

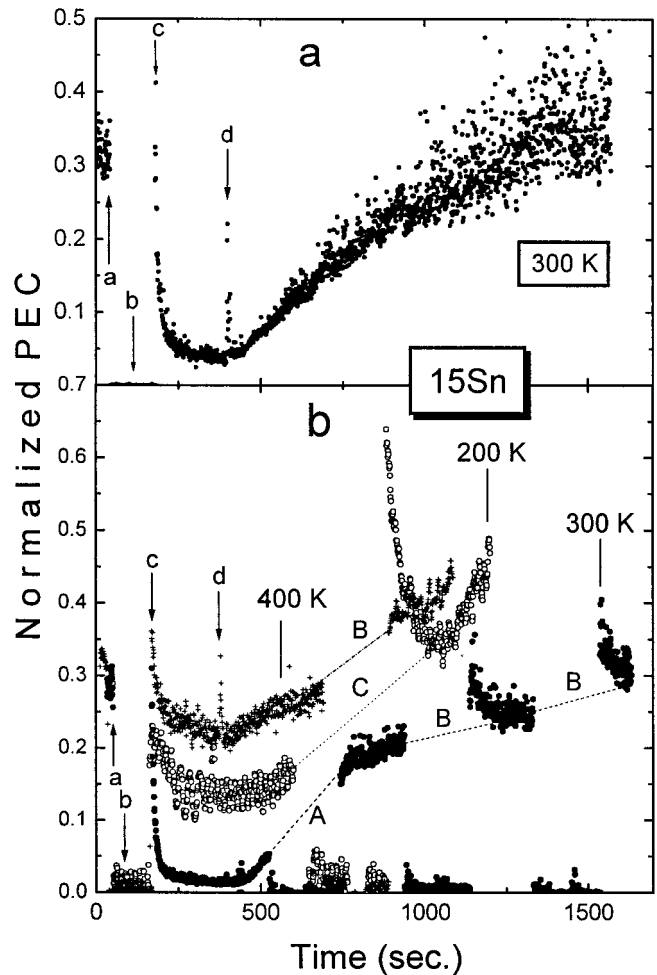


FIG. 8. Illustration of detrapping effects in sample 15Sn for O₂ admission. This entails PEC measurement of exposure sequences, following a saturation sequence of exposure to 30 Torr O₂. The PEC is normalized to the initial current before the saturation sequence; a—beam off; b—0.002 Torr; c—beam on; and d—pump-out. (a) Uninterrupted PEC recovery after pumping; (b) beam blocking and O₂ admission during the recovery: A—beam blocked (in vacuum); B—beam blocked + ~30 Torr O₂; C—beam blocked + 0.01 Torr O₂.

gas-exposure and illumination sequence and on exposure to oxygen of the residual PEC. Figure 7 presents a sequence of 0.01 Torr O₂ exposure on a 15Sn sample, performed at 400, 300, and 200 K. It can be observed that the initial PEC decrease and the residual PEC value are almost temperature independent. The accumulation effect, however, is maximum at 300 K. Figure 8 presents a 0.002 Torr O₂ exposure measurement, starting with a residual PEC (previously saturated by a high dose of oxygen and beam illumination). There is a slow recovery to the initial saturated PEC value in (a). In (b), for the measurement performed at 300 K, the beam was blocked for several periods. In period A (vacuum) the PEC recovery seems to be beam independent. In periods B, a high (~30 Torr) pressure oxygen was introduced into the vacuum system and pumped out before the beam was turned on. It can be observed that there is a small effect of the oxygen admission, i.e., the initial current (after turning the beam on) is somewhat higher and a slow decrease, like that of virgin PEC in vacuum, takes place. For 400 K, the PEC recovery is

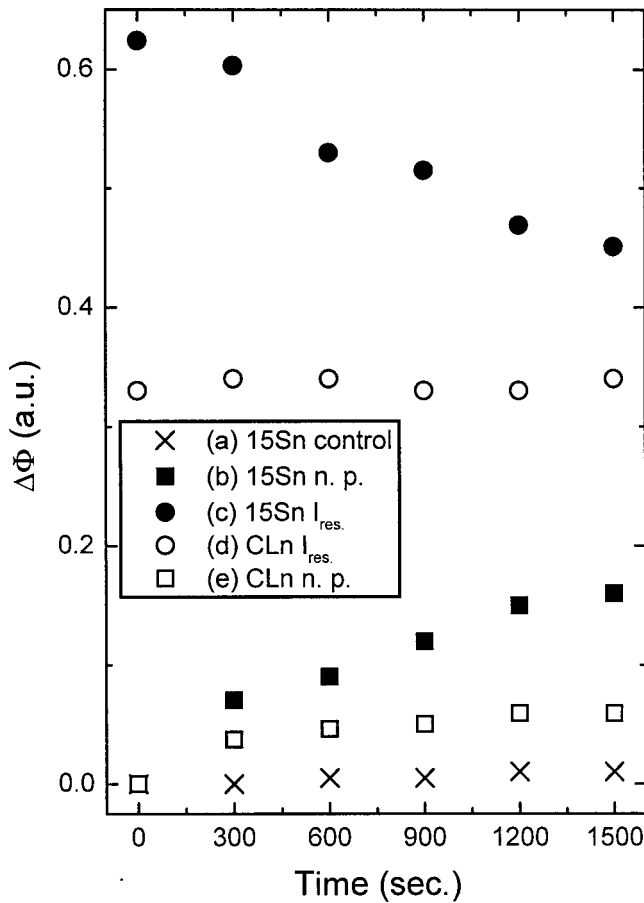


FIG. 9. Time dependence of the residual (saturated) PEC (transformed into WF, see Sec IV A). I_{res} , at an irradiation spot (a), PEC at a nearby ($\sim 100 \mu\text{m}$) point, n. p. (b), and a far ($\sim 1 \text{ mm}$) point (c) for both an oxide covered (15Sn) and clean Si (CLn) samples (d) and (e).

essentially beam and gas independent. For 200 K, only 0.02 Torr oxygen was admitted, but the effect of beam recovery, beyond the saturation value, and the following decrease are very pronounced.

As mentioned earlier, the effect of laser beam and gas exposure are largely confined to the measurement spot. To determine whether this is valid for longer times, a full O_2 exposure (and PEC measurement) sequence was performed on a 15Sn sample and the saturation value of the residual PEC was achieved. The illumination spot was then moved $\sim 100 \mu\text{m}$ away and the current measured for $\sim 20 \text{ s}$. The current was measured again at intervals of 5 min. A similar sequence of current measurements was performed on a spot $> 1 \text{ mm}$ from any former measurement. The same measurement sequences were performed after removal of the oxide (by heating). The normalized (to virgin) current intensities, transformed into effective WF changes (see Sec. IV A) versus time of the two sequences for both samples are presented in Fig. 9. Figure 10 depicts similar measurements performed at 200 K on a 15Sn sample for two spots, adjacent to the initially saturated PEC, I_{res} . For one spot the virgin PEC was lower than I_{res} and no change in current with time was obtained, while for the other, having a PEC higher than I_{res} there was a significant increase in WF with time. Also, no temperature effect on the rate of WF increase with time is

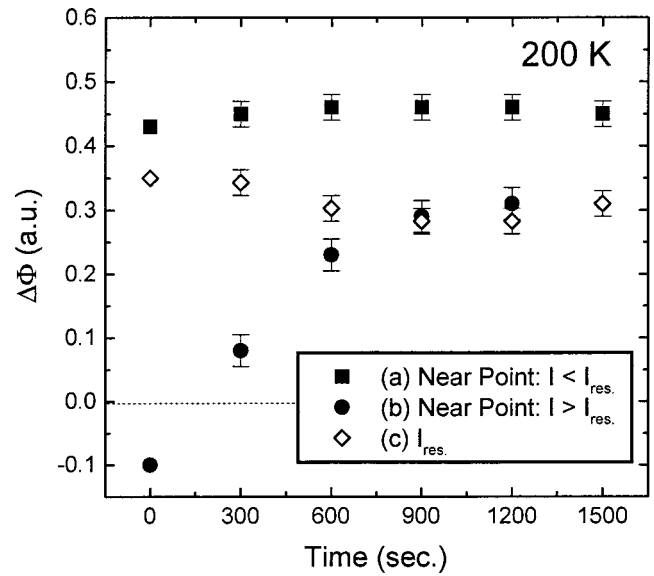


FIG. 10. Time dependence of the (a) residual PEC, (b) PEC at a near point where $I > I_{res}$, and (c) at a near point where $I < I_{res}$.

observed. Figure 11 presents a combined CPD and PEC measurement on a 15Sn sample for a 0.1 Torr exposure, in a sequence imitating the former PEC measurements (Figs. 5 and 6). It must be recalled that the vibrating KP disturbs the PEC measurement, so the measurement provides only the

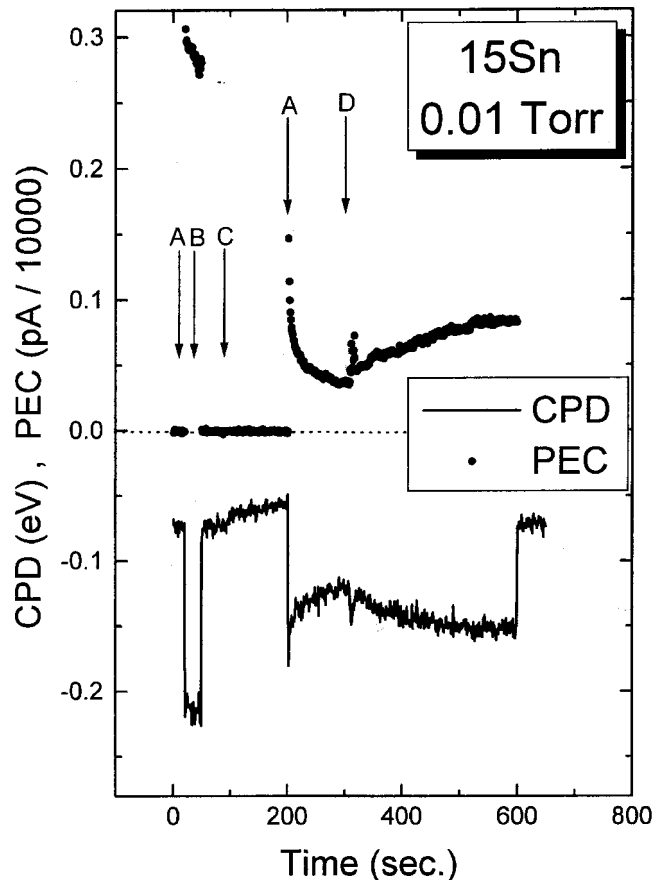


FIG. 11. A combined PEC and CPD measurement of a 0.1 Torr exposure sequences on a 15Sn sample. A—beam on, B—beam off, C—gas admission, and D—pumping.

qualitative behavior. It is observed that the CPD measurement is essentially a mirror image of the PEC experiment when the beam is on. This is not trivial to achieve since the CPD measurement is performed outside the irradiated area, at a distance of about 1 mm from the KP edge.

IV. DISCUSSION

The basic concepts related to MPPE from oxidized silicon have been discussed elsewhere. The PEC method uses the fact that the PEC (4PPE as well as 3PPE) magnitude is PEC strongly dependent on the photoelectron excess (kinetic) energy. The photoemission yield, Y_{PE} , changes through $\Delta\Phi$, the threshold energy change caused by the photoinduced charging, as²⁵

$$Y_{PE} \propto [n\hbar\omega - (E_T + \Delta\Phi)]^m, \quad (1)$$

where $n=3$ for 3PPE and 4 for 4PPE for photons of energy $\hbar\omega$; E_T is the energy separation between the Si VB and the vacuum level, while Φ is the separation between the Fermi level and the vacuum level. One usually takes $m=2$ in Eq. (1), consistent with photoemission dominated by bulk-state processes, except for very close to the threshold ($n\hbar\omega - \Phi < 0.1$ eV) where $m=3/2$.²⁵ We will take $m=2$ in what follows, since we expect $4\hbar\omega - \Phi = 6.2 - 5.15$ eV ~ 1 eV and $3\hbar\omega - (\Phi - E_g) = 4.65 - 4.05$ eV ~ 0.6 eV for 4PPE and 3PPE, respectively, where $E_g = 1.1$ eV is the Si band gap. Normalizing the yield to its initial (virgin) value, Y_0 , we obtain

$$I_n = \left[\frac{n\hbar\omega - (E_T + \Delta\Phi)}{n\hbar\omega - E_T} \right]^2, \quad (2)$$

where $I_n = Y/Y_0$. Hence (assuming that the PEC is a 4PPE process and $4\hbar\omega - E_T \approx 1$ eV)

$$\Delta\Phi = 1 - I_n^{1/2}. \quad (3)$$

Since the PEC is not purely a 4PPE process²¹ and $4\hbar\omega - E_T > 1$ eV, Eq. (3) is not accurate and only the functional dependence of $\Delta\Phi$ on I_n will be used. The units are arbitrary, although the values are not far from the actual eV values.

A general remark is in place here about the possibility of derivation of quantitative parameters from the MPPE as well as CPD results. These techniques are sensitive to the initial charging of traps on the one hand and trap density on the other hand, and both vary laterally (as will be discussed later). The inability to map these initial conditions (this could be achieved by a scanning Kelvin probe, not available in the present study) strongly cripples quantitative calculations. However, as can be seen in the following, distinction between trap families, the differentiation in their existence in the oxide and bulk and observation of processes of trap filling, gas-assisted and temperature-dependent detrapping and surface mobility of trap charges can be derived and is presented.

V. VACUUM DIRECT FILLING (DF) OF CHARGE TRAPS

In principle, vacuum transient surface charging is possible if it is confined to the irradiated spot area (therefore not

being monitored by KP). However, this is not plausible since for the gas-assisted surface charging there is a (Coulomb-repulsion driven) charge spillover from the irradiated spot, easily monitored by the KP (see Sec. III B). There is no reason why similar transient charging in vacuum should be bound to the irradiated spot in spite of the repulsion force. It is therefore concluded that transient charging does not take place in vacuum and the residence of gas on the surface is a precondition for this effect.

The residual low intensity of the PEC following its slow decrease in vacuum is stable for a long time after the beam is turned off and it is attributed to direct filling of charge traps by MPPE (as opposed to trap filling following gas-assisted surface charging).²¹ The DF process is not monitored by the CPD measurement, since it is confined to the irradiated spot. It is observed for all samples (Fig. 3), but not at all spots on a specific sample, and with parameters changing from spot to spot. Also surface treatment can change the specifics of the process (graphs 1 and 2 in Fig. 3 illustrate DF processes on the same sample, the second one after a few heating and cooling cycles to remove quasi-steady trapped charges). The strong diversity in the specifics of the DF process obscures the possible relevance of the thickness and nature of the oxide to the process.

The functional behavior of the time-dependent PEC may point to the specific process taking place. In order to learn about actual charge trapping via the changes in the threshold energy \sqrt{Y} has to be analyzed [Eq. (1)]. Most of the DF curves can be fitted with a two-exponent decay function. For a high-intensity beam (>20 GW/cm²), the fast decay time is in the range of tens to hundreds of seconds, while the slower one is >1000 s and up (see Figs. 3 and 4). This could point to the existence of either two different trapping processes and one family of traps, or to one process and two families of traps. Two processes could involve, e.g., 1PPEs and 2PPEs. For a family of identical traps, however, the ratio between the two processes should be constant for a particular experiment, but this is not observed. The possibility of two families of DF traps having different energy levels (so each can be filled by a different combination of MPPEs) and a diverse concentration across the sample seems to be more plausible. Most DF curves for the CLn and CLp samples (see Fig. 3, graphs 4 and 7) can be fitted with a single exponential with a long decay constant.

It is hard to draw quantitative conclusions from the intensity dependence of t_1 and t_2 in Fig. 4, since the different behavior at different spots is undoubtedly partially responsible. However, the trend seems to be that while t_2 corresponds to nearly linear dependence with laser irradiance, suggesting 1PPE filling, t_1 corresponds to a significantly higher power law, as would occur with MPPEs. Also, the faster decrease of A_1 , the preexponent of t_1 , relative to A_2 , is in accordance with MPPE. This implies that one family of DF traps lies low enough in energy above the Si VB to be filled with 1PPE, having a very low filling efficiency (long time constant), and the other family lies significantly higher in energy but has a much higher filling efficiency. Both trap families are present in both the oxide and the Si substrate, but, deduced from the CLn and CLp DF curves, the high-

energy family is present mostly in the oxide and not in Si. Both families are very diverse in absolute as well as relative trap densities.

For different spots there is a strong variation in the PEC current (up to an order of magnitude) and decay time constant. A variation in DF-trap density could account for different saturation magnitudes of the PEC decrease but not for the initial decrease rate (unless the density is practically zero at certain spots). A more plausible possibility, which can also account for the different initial values of the PEC and SH, is a diversity in the initial trap population. A locally DF trap-filled spot (prior to laser illumination) will not exhibit a DF-induced decrease of the PEC. A diversity in the initial filled-traps-induced electric field can also count for the diversity in PEC and SH intensities. Since the escape depth of the MPPE electrons is ~ 10 nm,²³ lateral variations in the oxide thickness do not play a significant role in the variation of current intensity. However, defects/voids in the oxide may cause local variations in initial trap filling. A significant, long living, diversity in initial charging of Si/SiO₂ is consistent with scanning KP measurements.²⁶ Measuring the PEC yield at a DF saturated spot tens of minutes after the illumination was stopped revealed no significant change. Thus no mobility of charges in DF traps was detected.

A. Photon-induced gas-assisted charging (PIGAC)

After gas removal in an illumination and exposure sequence (Figs. 5 and 6), the PEC reaches a value significantly lower than the initial one. It is believed that this decrease in PEC (and consequent increase in WF) is caused by transfer of surface charge to long lifetime traps, analogous to the DF process occurring in vacuum. Before embarking on detailed explanations we offer the following qualitative comments: (1) As can be observed in Fig. 5, the residual current reaches a steady state and no apparent DF process can be observed following pumping, even after a short exposure dose. Hence the surface charge transfer to long lifetime traps includes filling of the DF traps (much more efficiently than the DF process). (2) The saturation PEC value reached after oxygen exposure, for all the oxide covered samples, is significantly lower than the residual current reached in vacuum [marked in Fig. 5(b)]. Therefore, different families of slow traps are assumed for the DF process alone (DF long lifetime traps) and for PIGAC transformed to charge trapping, hence gas-sensitive (GS) long lifetime traps (this process includes filling of the DF traps). For the CLn and CLp samples the saturation value seems to be well within the range of the DF saturation, so only DF traps are assumed to exist in the Si substrate (at the Si/SiO₂ interface). (3) As stated earlier (Sec. III A) the residual current is lower after several heating/cooling cycles, indicating the formation of charge traps in the cooling/heating process. (4) The recovery time of the PEC, reaching a saturation value following pumping, decreases with pressure from 80 to 30 s for the oxide covered samples and increasing with pressure from 3 to 8 s for the CLn and CLp samples (Fig. 5). This is qualitatively correlated with desorption times of oxygen measured for these samples by the KP (not shown). It is concluded, therefore,

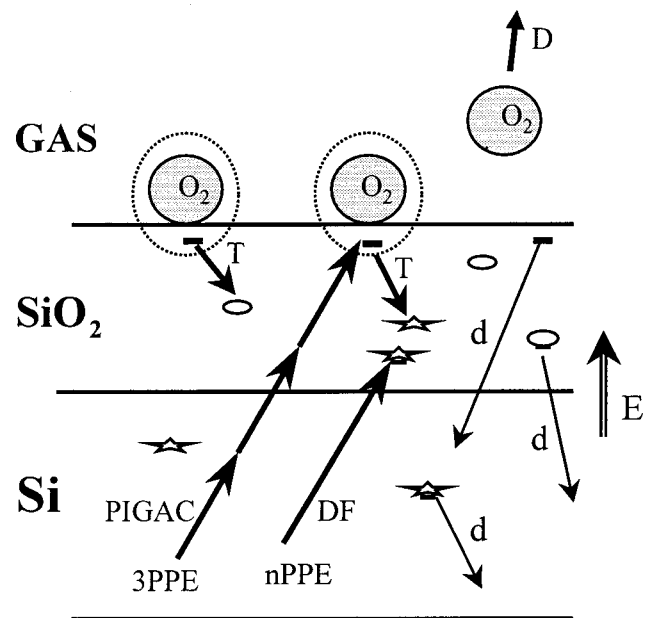


FIG. 12. A schematic presentation of the proposed model for traps and charge transition processes. nPPE represents the variety of single and multi-photon-photoemission DF processes. A star denotes DF traps (DF+PIGAC filled), an ellipse denotes GS traps (PIGAC filled). E—PIGAC induced electric field, T—trapping, D—desorption, and d—dissipation.

that this behavior is controlled by the different mechanisms of desorption from the oxide and clean Si surfaces, which is beyond the scope of the present study. (5) The sharp drop in PEC, following gas+beam exposure, seems to be the feature least affected by the specific choice of working spot. All other quantities are affected, some more than others, adding to the spread in results beyond the statistical measurement error, and also making it harder to compare measurements performed with different techniques, or using the same laser conditions but on different spots.

The sharp pressure-dependent drop in the PEC observed in Fig. 5 (as well as the rise in the EFISH signal^{8,11,21}) is attributed to oxygen field-induced adsorption, discussed elsewhere,²⁷ combined with PIGAC of the surface.^{8,11,27} The gradual decrease of the PEC that follows, ending in a steady state current, is attributed to the combination of surface charge accumulation and trap filling. The gradual increase (decrease) of the residual current (EFISH signal) to a steady-state value is attributed to desorption of the oxygen species from the surface (together with charge dissipation for the gas-attached electrons). This is combined with a (longer time) detrapping process that is different for different types of samples studied (Fig. 6). The model proposed is schematically presented in Fig. 12. For simplicity, a single symbol and a single filling process are assigned to the DF traps, though it was deduced that there are at least two trap families, having different filling processes and distributions. The processes, as can be observed, are interconnected. Too many parameters are unknown and therefore a complete mathematical presentation is complicated and an exact solution is impossible. However, the charging/filling seems to be exponential like, so effective time constants can be measured for the different processes and in principle their dependence on

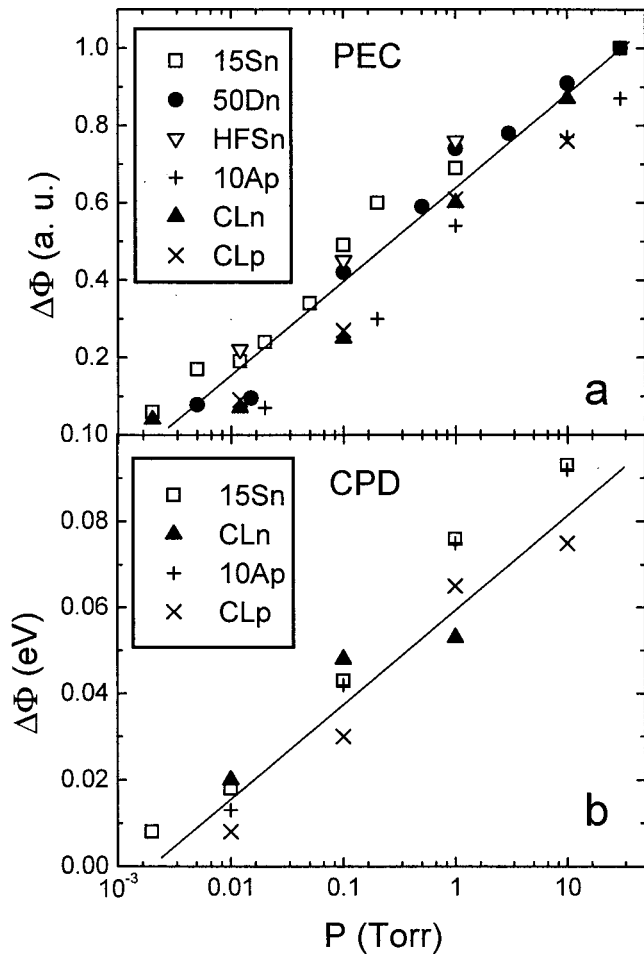


FIG. 13. (a) The initial decrease of PEC (normalized to the initial value), following oxygen admission for the various samples. The line is just a guide to the eye. (b) Kelvin probe measured pressure dependence of the (reversible) WF change of adsorbed oxygen for two oxide covered samples and the same samples after oxide removal.

the experiment parameters (e.g., pressure, dose) can be deduced.

Figure 13(a) presents the initial PEC decrease following various oxygen doses, expressed as work function (WF) changes according to Eq. (1). The KP was used to measure the adsorption of oxygen on the various samples. The WF changes induced by this adsorption are presented in Fig. 13(b). All samples show a $\log(P)$ behavior having about the same P dependence, both for the PEC and CPD results. As was proposed,²⁷ the $\log(P)$ dependence of both the adsorption and the charging-induced PEC decrease points to a linear relation between the amount of adsorbed oxygen species and the surface transient charge, leading to the suggestion that the photoinjected electron is electrostatically coupled to an oxygen molecule, thereby creating an additional transient adsorption site. This coupling also transiently traps the photoelectron on the surface, leading to PIGAC. Since oxygen is the only adsorbate causing a strong accumulation effect via PIGAC, it was suggested that the adsorbed O_2 molecules combine with the surface electrons to form metastable O_2^- species²⁸ on the surface. A balance is achieved for other gases²⁷ by this coupling to the adsorbates on one hand, and desorption causing electron dissipation and charge transfer to

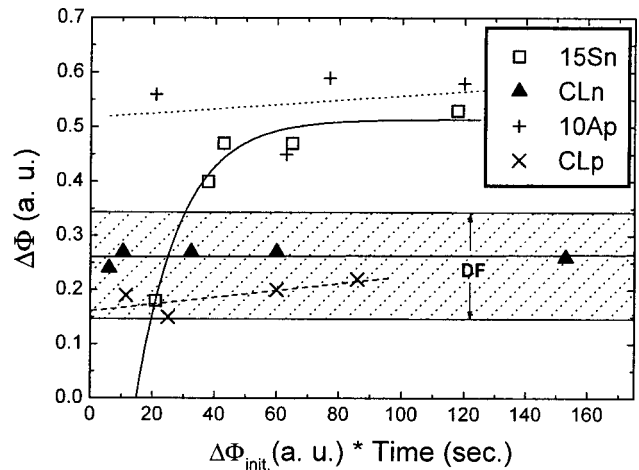


FIG. 14. Charge dose (defined in the text) dependence of the WF change due to charge trapping (monitored by the residual PEC) for the oxide covered (15Sn, 10Ap) and clean Si (CLn, CLp) samples. The dashed area denotes the WF changes for CLn and CLp due to the DF process.

traps on the other hand. O_2^- , being metastable,⁴ causes the strong pressure-dependent accumulation of surface charge. Accumulation is almost nonexistent at 400 K, but this is not surprising since the lifetime of surface O_2^- is expected to decrease. However, accumulation is also not significant at 200 K, where it could be expected to be stronger than at 300 K. This may be the result of the existence of two potential wells for surface oxygen species.²³ The 10Ap, CLn, and CLp present [Fig. 13(a)] somewhat lower PIGAC values, probably due to the type of oxide for the first one, and the lack of oxide for the others.

B. Filling of gas-sensitive (GS) long-living traps

The residual PEC, being lower than the initial value, is believed to be the result of trap filling, mainly by transfer of PIGAC electrons to long lifetime traps combined with DF (see Fig. 12). The evaluation of the dose of surface charge (a fraction of which is transferred to the traps), which should be the integral of instantaneous surface charge over the gas+beam illumination time, is not trivial. Since the decrease in PEC, following the initial step, is due to a combination of surface charge accumulation and trap filling (that does not contribute to the dose), they are not easily separated. An effort to separate the two contributions was made by using measurements performed on trap saturated spots [e.g., Fig. 8(a)] in which only surface charge accumulation is present. The diversity of initial conditions attributed to initial trap filling (Sec. IV A) affects the distribution of time constants of the PEC decrease, so the separation of the contributions is impossible. The dose was therefore defined as the initial WF decrease (due to PIGAC) multiplied by the exposure time, taking into account that the surface charge accumulation is also proportional to the charging rate (initial PEC decrease).

The normalized value of the residual current (following the pumping of the gas), translated to $\Delta\Phi$, is presented in Fig. 14 for the oxidized as well as the CLn and CLp samples versus the dose of PIGAC. For the 10Ap, CLp, and CLn

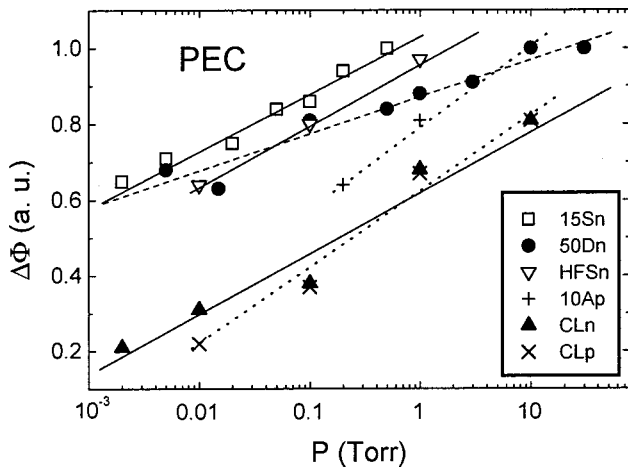


FIG. 15. The pressure dependence of the WF changes monitored by saturation PEC upon oxygen exposure of the various studied samples.

samples the residual current is almost dose independent, i.e., the efficiency of trap filling for these samples is very high and they are filled by a small dose. The efficiency for 15Sn seems to be lower by at least an order of magnitude, maybe due to the specific oxide covering the sample. Also, as in Fig. 5, it can be seen that the range of saturated charge traps for the clean Si samples lies within the range of the DF traps, leading to the conclusion that only DF traps are present in Si and the GS ones are confined to the oxide.

The pressure dependence of the saturation values of the (normalized) PEC decrease, in the presence of oxygen with the beam on, is presented in Fig. 15. All samples except 10Ap, CLp, and CLn seem to have similar saturation values (with slightly different pressure dependencies, the significance of which is unclear) and 10Ap exhibits slightly lower values. The values for CLp and CLn are significantly lower, with each sample presenting similar pressure dependence to its oxide covered counterpart. Since the decrease in PEC, following the initial step, is due to a combination of PIGAC and trap filling, a lower PIGAC efficiency [for 10Ap, exhibited in Fig. 13(a)] is a possible cause for the lower saturation value. Another possible contributor may be (since the PEC saturation is a combination of surface charging and trap filling) a different trap density, namely the lack of GS traps for CLn and CLp and a possible lower trap density in the oxide of the 10Ap sample. It can be seen that though there is some (probably spot related) spread in the values, the $\log(P)$ dependence is quite clear, in accordance again with adsorption of charged particles (Fowler–Guggenheim isotherm).

After saturation of the long lifetime traps by a high dose of oxygen [Fig. 8(a)], the decrease in the PEC due to gas+beam exposure is due only to PIGAC. Because of the long lifetime, and in the case of the 15Sn and other samples the residual PEC reaches a steady state, the decay of the surface charge in Fig. 8(a) is due to the combination of oxygen desorption and charge dissipation. It has to be considered that desorption of even the relatively stable O_2^- is expected to be much faster than a few mixtures.⁴ Also, no O_2 was observed minutes after pump-out (much shorter than the dissipation time of the residual effect), when the sample was

heated in front of the mass spectrometer. The long recovery time is probably due to slow charge dissipation from traps that were filled by the additional exposure to 0.002 Torr and will be discussed in Sec. IV E. Fitting a double exponential decay [not surprising considering the complexity of the interconnected processes that are taking place (Fig. 12)] to the PEC decrease of Fig. 8(a), we obtain time constants $\tau_1 \sim 6 \pm 2$ s and $\tau_2 \sim 40 \pm 5$ s. However, the values derived from the fits to the same PEC decrease following an exposure on a virgin spot, or a DF saturated one are $\tau_1 \sim 5 \pm 3$ s and $\tau_2 \sim 30 \pm 15$ s. It can be concluded that the PIGAC process is dominant when it occurs together with GS charge trapping, so the difference in the time constant between the process including trapping or excluding it is negligible. Furthermore, the diversity in the initial trap charging conditions (Sec. IV A) causes a position-dependent WF that affects the PIGAC process significantly.

Checking the pressure dependence of the PIGAC effective time constants (not presented), a general trend of a shorter time with increasing pressure is obvious. On the other hand, the spread of the results caused by the position dependence prevents a more specific analysis from which more physical parameters and a better understanding of the process could be achieved.

C. Surface-charge mobility (spillover)

As indicated in Sec. II, the KP is not sensitive to processes that are limited to the area of the beam illumination. Figure 11, in which the CPD changes are correlated to the PEC ones, proves that charge spillover from the irradiated spot to a significantly larger area (possibly the whole surface) occurs. In contrast to a similar spillover occurring for H_2 , He, and CO ,²⁹ the CPD for oxygen is a mirror image of that of the PEC during the PIGAC and also during the pumping and detrapping. This indicates that the charging of the whole surface closely follows that of the irradiated spot, or, in other words, the spillover is fast. This is caused by the oxygen-induced charge accumulation on the irradiated spot creating a high charge concentration compared to other gases and a stronger Coulomb-repulsion serving as the driving force for spillover. The spillover is probably of the coupled electron-gas species, thus the PEC recovery is controlled by the gas desorption which affects the CPD outside the irradiated spot in the same way it affects the PEC inside the spot. For 1–10 Torr (not presented) charge transfer accumulation induces a CPD increase of the order of $\Delta\Phi = 0.1$ eV. For the 1.5 nm oxide of 15Sn the maximal near interface electric field is (assuming it is across the oxide) 0.6 MV/cm. Taking the oxide relative dielectric constant to be 3.8, we estimate from Gauss' law that the surface charge density is $\sim 1 \times 10^{12}$ electrons/cm².

D. The residual PEC and detrapping

The residual PEC after the gas has been pumped out reflects the fraction of traps that had been filled by the combination of transfer from PIGAC and DF (in addition to the initially full ones). Detrapping should affect both the PEC and CPD in the same way. Figure 11 (which presents a CPD

measurement outside the irradiated spot) proves that desorption as well as detrapping is essentially irradiation independent. For the detrapping this is in accordance with Fig. 8(b) in which the rate of PEC recovery seems to be beam independent. Figure 6 presents very different time dependencies of the PEC recovery following the gas pumping for the different samples. It can be seen that for the clean Si samples the PEC reaches a steady state immediately after pump-out. Recalling that for these samples the residual PEC is considered to be due to filling of only DF traps (Sec. IV C), this is in accordance with the fact that no mobility was measured for the DF traps (filled directly in vacuum. Sec. III A). While for 15Sn a pseudo-steady state (see mobility measurements, Fig. 9) is achieved in a few tens of seconds; for 50Dn and 10Ap it takes ~ 500 s (not shown) and for HFSn no steady state was measured for many minutes (the specific contribution of trapped charge mobility has not been measured for all the samples). The accelerated recovery of the PEC for HFSn (being a sample with a very thin and damaged oxide, following partial etching) points to charge dissipation. This is probably due to the fact that most oxide traps lie close to an interface (either with the Si or with the surface) which supplies a detrapping route.

In Fig. 8 beam+oxygen exposures on a beam+oxygen saturated spot are presented. Since the GS and DF traps are already saturated before the addition of the beam+0.002 Torr O_2 , the decrease in PEC with the beam+gas on is supposedly due to PIGAC only. After pumping the gas out, however, the PEC recovery should have been much faster [~ 200 s, a typical desorption time, see Fig. 5(a)]. The slow (~ 1000 s) recovery time points to charge traps (having a shorter life time than most GS traps—see Fig. 9) that were not full when saturation was achieved. It is not likely that a beam+0.002 Torr O_2 combination can fill traps that were not filled by a beam+30 Torr one. It seems therefore that together with the PIGAC and the efficient charge transfer to traps, there is a gas-dependent detrapping mechanism (at least for part of the traps) having different pressure dependencies than the PIGAC. For a few cases of the sequence presented in Figs. 5 and 6, for gases different than oxygen, the residual current was higher than the initial one.²⁹ This can be attributed to a detrapping process that was for the specific measurement more efficient than the transfer of PIGAC charge to traps.

The 300 K measurement in Fig. 8(b) presents the same process as in Fig. 8(a), except the beam is blocked for a few 100 s periods. It exhibits the independence of the detrapping process on the beam irradiation (except for the fast increase when the beam is turned on that might be due to heating to the steady state temperature). When ~ 30 Torr O_2 is added when blocking the beam, it can be observed that a small amount of detrapping occurs and the DF process resumes. It seems that the gas detrapping is most effective on the DF traps and it can be assumed that the gas affects the high-energy (shallow energy well) DF family (see Sec. IV A). The quantitative irreproducibility of the gas detrapping, especially for the other gases, still requires extensive experimental study and analysis in order to clarify and hopefully quantify this effect. The 400 K and 200 K measurements of this

detrapping effect demonstrate its strong temperature dependence. While for 400 K the recovery of PEC seems to be unaffected by the admission of 30 Torr of oxygen, for 200 K the admission of only 0.01 Torr causes significant detrapping and resumption of a strong DF process. It is likely that this large enhancement with temperature decrease is caused by the prolonged presence of gas molecules (adsorbed or in the gas phase) on the surface.

It should be noted that while the CPD change following the desorption is due to charge dissipation from the surface (detrapping), for the PEC also a mobility of trapped charges from the illuminated spot outwards should contribute. The similar time constants for both CPD and PEC in Fig. 11 demonstrates that the latter is slower than the detrapping so it does not affect the total time constant significantly.

E. Mobility of trapped charges

Figure 9 (described in Sec. III B) presents the mobility of the trapped charges. The slow increase of the PEC following the short-time steady state achieved for 15Sn [Fig. 5(a)] has indeed a significant detrapping component. On the other hand, the increase of PEC (decrease of WF) at the nearby point (compared to the steady PEC of the control point) is mostly a result of charge mobility from traps in the irradiated spot to nearby empty traps, with a small contribution of DF. A comparison to the clean Si measurements shows that there is no residual PEC increase at the irradiated spot. This is in agreement with the finding for the DF reduced PEC that there is no mobility from the DF traps (Sec. IV A) and with the conclusion that only DF traps are present in the Si substrate (Fig. 14). The small PEC decrease (WF increase) at the nearby spot can therefore originate only from DF, which is probably stronger at this specific spot than at the control point of the 15Sn sample. Figure 10 (200 K) demonstrates that the mobility of trapped charges is Coulomb repulsion driven rather than thermally driven. There is a clear mobility from a spot with high trap-charge density (filled by beam irradiation) to a less densely charged spot (higher initial PEC). In contrast, there is no mobility at all to a more densely charged spot (higher “virgin” density, i.e., initial PEC lower than that of the residual one at the irradiated spot).

VI. SUMMARY AND CONCLUSIONS

The combination of PEC and CPD has been applied to study the effect of laser beam irradiation of various Si(001)/SiO₂ in vacuum. Both techniques were found to be $\sim 10^3$ times more sensitive than EFISH to changes in the WF due to adsorption and charge transitions on the surface and in the Si/SiO₂ interface. This enabled a detailed study of the various effects of photon-induced gas-assisted charging as well as charge transfer to long lifetime traps, directly by internal photoemission in vacuum or via the surface transient charging in the presence of ambient oxygen.

Various samples of different doping, oxide preparation, and oxide thickness as well as clean Si(001) samples were studied. It appears that the (low) doping level does not seem to be a relevant parameter and the different oxides only in-

significantly change the efficacy of charge trapping. For all the samples, the surface charging is similar and is believed to obey a universal mechanism of electrostatic electron-molecule coupling.²⁷ No transient charging was detected in vacuum. Charge accumulation during the continuous irradiation in the presence of ambient oxygen is believed to be due to the formation, in a second step, of metastable O_2^- on the surface. This charge accumulation was found to be very effective at 300 K, but almost not present at 400 K as well as 200 K where the stability of O_2^- should be increased. The temperature dependence of this effect should be further studied in detail. At this time, it is proposed that the formation of O_2^- on the surface may be mediated by phonons, which may explain the less efficient accumulation at 200 K. A fast, Coulomb-repulsion-driven, spillover of surface charge from the irradiated spot to the rest of the surface was detected.

Transfer of electrons to long lifetime charge traps was detected in vacuum by the time-dependent decrease in intensity of the PEC. It is assumed that direct filling of traps by internal photoemission takes place. Two distinct exponential decay processes were observed for high power (≥ 20 GW/cm⁻² peak power) measurements on oxide covered samples. For the clean oxide samples and for low power excitation, the PEC curves could be fitted with one exponent. This leads to the conclusion that there are at least two trap families, filled by the DF process. The first one, having an energy low enough to be filled by photoelectrons absorbing one photon, is present in the oxide as well in the Si substrate. The second family is filled only by multiphoton absorbing photoelectrons and is present mostly in the oxide. Transfer of the transient (ambient oxygen-assisted) surface charge to the DF traps was found to be significantly more efficient than the DF process. In addition another family of charge traps, filled only in ambient oxygen (or other gas²⁹) presence, was detected. This family of traps is present only in the oxide. The efficacy of filling of the gas-sensitive traps seems to depend on the specifics of the oxide for various samples. Since the residual PEC after gas removal, for the clean Si samples, was always in the range reached by the DF process, it is assumed that only DF traps are present in the bulk Si.

There are significant differences in PEC initial value as well as in the specifics of the DF process when moving from point to point across the surface. This leads to the conclusion that there is a strong diversity in the initial density of filled traps, i.e., some of the traps are initially filled even following a heating (detrapping) treatment. This diversity affects the specifics of all charging and trapping processes and makes any quantitative analysis difficult.

Charge mobility of the trapped electrons was measured by monitoring the change in PEC over tens of minutes at an irradiation and oxygen exposure saturated spot and adjacent (~ 100 μ m away) spots. No charge mobility was detected following the DF process. Also, no charge mobility was detected for clean Si samples, in accordance with the assumption that only DF traps are present there. For the oxide-covered samples a clear mobility was detected, supposedly hopping between traps. Looking at a spot for which the initial PEC was lower than the saturated one for the adjacent spot, no mobility was detected in that direction. This proves

that the mobility of trapped charges is driven by the Coulomb repulsion between the electrons and also supports the concept of lateral variation of initial charging of charge traps, in which no mobility is possible from a less to a more charged region.

Detrapping of electrons from the long lifetime traps can be obtained by spontaneous dissipation (possibly also by hopping to an easier to detrap region), observed in the process of increasing residual PEC for some samples, especially the one partially etched by HF. The oxide of this sample is thin and rough, so every volume in it is close to either the vacuum or the Si interface. Another route of detrapping is via ambient oxygen (beam blocked), which causes no detrapping at 400 K, a small effect of detrapping at 300 K, and a dramatic enhancement of the effect at 200 K. At least part of the electrons that get detrapped are from DF traps since the DF process is observed following the detrapping. Another proof that gas-induced detrapping takes place is that when a spot that was saturated by 30 Torr O_2 and beam illumination is exposed to 0.002 Torr O_2 +beam, the PEC is further reduced. The recovery time to the former saturation value is much longer than the desorption time of the gas from the surface. This means that saturation was not full due to simultaneous detrapping by the ambient gas. Probably the pressure dependencies of trapping via surface charging on one hand and detrapping on the other hand are so different that an addition of 0.002 Torr O_2 in the presence of irradiation can add trapped charge to the spot affected by 30 Torr O_2 exposure.

ACKNOWLEDGMENT

We gratefully appreciate financial support from the Natural Sciences and Engineering Research Council of Canada and Photonics Research Ontario.

- ¹E. Takeda, C. Y. Yang, and A. M. Hamada, *Hot-carrier Effects in MOS Devices* (Academic, San Diego, 1995).
- ²E. M. Allegretto and J. A. Bardwell (unpublished).
- ³T. K. Whidden, P. Thanikasalan, M. J. Rack, and D. K. Ferry, *J. Vac. Sci. Technol. B* **13**, 1618 (1995).
- ⁴H. Richter, T. E. Orłowski, M. Kelly, and G. Margaritondo, *J. Appl. Phys.* **56**, 2351 (1984); T. E. Orłowski and D. A. Mantell, *ibid.* **64**, 4410 (1988).
- ⁵C. Svensson, in *The Si-SiO₂ System*, edited by P. Balk (Elsevier, Amsterdam, 1988), p. 221.
- ⁶D. J. DiMaria, E. Cartier, and D. Arnold, *J. Appl. Phys.* **73**, 3367 (1993).
- ⁷G. Lüpke, D. J. Bottomley, and H. M. van Driel, *Phys. Rev. B* **47**, 10389 (1993).
- ⁸J. Bloch, J. G. Mihaychuk, and H. M. van Driel, *Phys. Rev. Lett.* **77**, 920 (1996).
- ⁹J. G. Mihaychuk, J. Bloch, Y. Liu, and H. M. van Driel, *Opt. Lett.* **20**, 2063 (1995).
- ¹⁰J. F. McGilp, *Prog. Surf. Sci.* **49**, 1 (1995).
- ¹¹N. Shamir, J. G. Mihaychuk, and H. M. van Driel, *J. Vac. Sci. Technol. A* **15**, 2081 (1997).
- ¹²O. A. Aktsipetrov, A. A. Fedyanin, E. D. Mishina, A. A. Nikulin, A. N. Rubtsov, C. W. van Hasselt, M. A. C. Devillers, and T. Rasing, *Phys. Rev. Lett.* **78**, 46 (1997).
- ¹³J. I. Dadap, X. F. Hu, N. M. Russell, J. G. Ekerdt, J. K. Lowell, and M. C. Downer, *IEEE J. Sel. Top. Quantum Electron.* **1**, 1145 (1996).
- ¹⁴U. Emmerichs, C. Meyer, H. J. Bakker, H. Kurz, C. H. Bjorkman, C. E. Shearon, Jr., Y. Ma, T. Yasuda, Z. Jing, G. Lucovsky, and J. L. Whitten, *Phys. Rev. B* **50**, 5506 (1994).
- ¹⁵C. Meyer, G. Lüpke, U. Emmerichs, F. Wolter, H. Kurz, C. H. Bjorkman, and G. Lucovsky, *Phys. Rev. Lett.* **74**, 3001 (1995).

- ¹⁶C. W. van Hasselt, M. A. C. Devillers, T. Rasing, and O. A. Aktsipetrov, *J. Opt. Soc. Am. B* **12**, 33 (1995).
- ¹⁷J. I. Dadap, X. F. Hu, M. H. Anderson, M. C. Downer, J. K. Lowell, and O. A. Aktsipetrov, *Phys. Rev. B* **53**, R7607 (1996).
- ¹⁸P. Godefroy, W. de Jong, C. W. van Hasselt, M. A. C. Devillers, and T. Rasing, *Appl. Phys. Lett.* **68**, 1981 (1996).
- ¹⁹A. Nahata, T. F. Heinz, and J. A. Misewich, *Appl. Phys. Lett.* **69**, 746 (1996).
- ²⁰C. Sebbene, D. Bolmont, G. Guichar, and M. Balkanski, *Phys. Rev. B* **12**, 3280 (1975).
- ²¹J. G. Mihaychuk, N. Shamir, and H. M. van Driel, *Phys. Rev. B* **59**, 2164 (1999).
- ²²See, for example, D. P. Woodruff and T. A. Delchar, *Modern Techniques of Surface Science*, 2nd ed. (Cambridge U.P., Cambridge, 1994), Chap. 7.5.
- ²³See, for example, A. Zangwill, *Physics at Surfaces* (Cambridge U.P., Cambridge, 1988), p. 21.
- ²⁴“S” probe controlled by a 07 Kelvin Probe Controller, produced by Besocke Delta Phi, GMBH.
- ²⁵E. O. Kane, *Phys. Rev.* **127**, 131 (1962); G. W. Gobeli and F. G. Allen, *ibid.* **127**, 141 (1962).
- ²⁶G. H. Brugging and I. D. Baikie, Proceedings 2nd International Symposium on Ultra-clean Processing of Silicon Surfaces (UCPSS '94), 1994, p. 193.
- ²⁷N. Shamir, J. G. Mihaychuk, H. M. van Driel, and H. J. Kreuzer, *Phys. Rev. Lett.* **82**, 359 (1999).
- ²⁸P. J. Caplan, E. H. Poindexter, and S. R. Morrison, *J. Appl. Phys.* **53**, 541 (1982).
- ²⁹N. Shamir and H. M. van Driel, *J. Appl. Phys.* **88**, 909 (2000).